Computed Tomography Beam Hardening Correction Based on Non-linear Segmentation

Xiaoke Zhang[1], Linyan Xue[1], Kang Yin[1], Tianyi Wang[2], Kun Yang[1*]

[1]*College of Quality and Technical Supervision*
Hebei University
Baoding, China
E-mails: 1254395643@qq.com, lyxue@hbu.cn, 1182856376@qq.com, hbuyangkun@163.com

[2]*China Association for Standardization*
Beijing, China
E-mail: wty@china-cas.org

[*]*Corresponding author*

Received: October 26, 2018 **Accepted: January 08, 2019**

Published: March 31, 2019

Abstract: *This paper aims to eliminate the hardening artifacts in computed tomography (CT) images caused by the polychromatic X-ray spectrum. To this end, a polynomial fitting correction method using non-liner segmentation method was developed through projection space optimization for single medium (water) and the mixed media (water-bone), and verified through simulation and phantom experiments. Unlike the traditional image space optimization strategies, the proposed method has low computing load and few noises, and only requires a one-off image reconstruction to remove the hardening artifacts. The experimental results show that the proposed method can remove CT hardening artifacts and improve the accuracy of image reconstruction, indicating that the project space-based correction method based on non-liner segmentation method can effectively eliminate artifacts and restore the true CT values.*

Keywords: *Computed tomography, Beam hardening correction, Projection space.*

Introduction

When subjected to X-ray irradiation, an object could absorb the radiation and weaken the X-rays passing through it, making X-ray irradiation a possible way to reflect the internal distribution of the object. The initial intensity I_0 and the intensity after passing through the object I of a monochromatic ray obey the Beer-Lambert law [11]:

$$I = I_0 exp\left(-\int_0^D \mu(x, y)\, dL\right), \tag{1}$$

where $\mu(x, y)$ is the linear attenuation coefficient of the material; L is the thickness of the target object.

However, the X-ray tube output of most commercial computed tomography (CT) scanners has a broad energy spectrum, which obeys the distribution $S(E)$ [10]. The typical energy spectrum distribution is shown in Fig. 1.

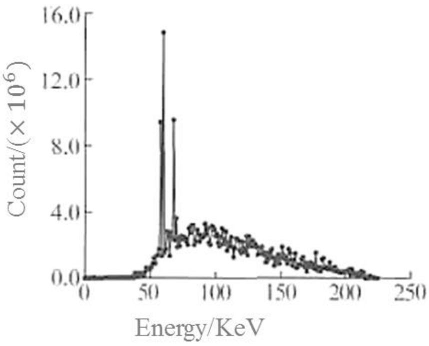

Fig. 1 X-ray energy spectrum distribution

In general, X-rays often form a polychromatic spectrum, where the total attenuation is a superposition of various exponentials rather than follow the simple exponential law [2]. The radiation attenuation can be expressed as:

$$I = \int_{E_{min}}^{E_{max}} S(E) exp\left(-\int_{0}^{D} \mu(x, y, E) dL\right) dE, \tag{2}$$

where E is the photon energy.

The polychromatic projection data can be expressed as:

$$q = \ln \frac{I_0}{I}. \tag{3}$$

Because of the negative correlation between $\mu(x, y, E)$ and E, the projection data q no longer changes linearly with the thickness of L (the result of computer emulation which is the lower curve in Fig. 2). In this case, the direct reconstruction of the collected projection data q may lead to cupping artifacts or other artifacts [10].

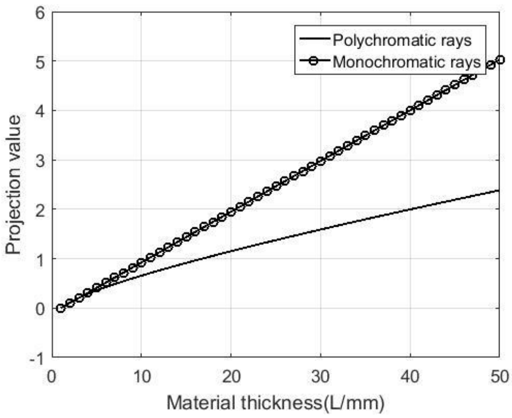

Fig. 2 The relationship between beam projection and penetration thickness

Many beam hardening methods have been developed to correct the artifacts. Among them, the dominant ways are hardware correction and software correction.

Ranging from water bag method to filter method [3, 4], hardware correction cannot efficiently utilize rays or completely eliminate hardening. Similarly, most software correction approaches have certain defects. For instance, the dual energy correction [5, 6], a complicated method, increases the radiation dose for the patient. Based on Nalcioglu's hypothesis [7], the single-energy method becomes too complicated when the material contains many substances. The iterative correction [9, 13] is not widely adopted due to the heavy computing load and slow reconstruction. Nevertheless, polynomial fitting enjoys great popularity thanks to its simplicity, ease of operation and excellent effect. In references [1, 2], this strategy is employed to construct a polynomial equation with the segmented images of different tissues as independent variables. When the total variation (TV) is the smallest, the coefficient can be solved at the cost of high computing load.

Inspired by the polynomial method, this paper attempts to set up a polynomial equation in the projection space and solve the coefficient by least squares method. Compared with that in reference [2], the proposed method only needs to reconstruct one image and features simple, fast solution and good correction effect.

Materials and methods

Hardening correction of cupping artifacts

The author put forward a single-energy approximation polynomial fitting method through the following steps.

Construction of an ideal model. The water image was extracted by binarization method and an ideal projection model Q, i.e., the projection space, was constructed through Radon transform.

Construction of a correction model. In the projection space, a correction model was built using the polynomial fitting form. The main idea is to obtain the equivalent monochromatic projection p_{final} through the polynomial combination of the polychromatic projection data q. The p_{final} can be obtained as follows:

$$p_{final} = \sum_{0}^{N} c_n q^n, \tag{4}$$

where p_{final} is the corrected projection; c_n is the corretion coefficient. When $N = 4$, Eq. (4) can be rewritten as:

$$p_{final} = c_0 q^0 + c_1 q + c_2 q^2 + c_3 q^3 + c_4 q^4. \tag{5}$$

Determination of unknown coefficients. In the projection space, the above correction model was compared with the ideal model. The coefficients were determined when the difference was minimal between the two models.

$$E = \sum \left(p_{final} - Q \right)^2 \to min. \tag{6}$$

In this case, the following formula is valid:

$$\boldsymbol{c} = H^{-1} \boldsymbol{a}. \tag{7}$$

Substituting the coefficient c_n into Eq. (4), we have the corrected projection. Then, the image without hardening artifacts can be obtained through reconstruction.

Hardening correction for streak artifacts

The proposed polynomial fitting method was applied to treat a case of dual media (water, bone). The main steps are as follows.

Image segmentation. The CT image was segmented by a nonlinear segmentation method [8]. The weight function distribution is described in Fig. 3.

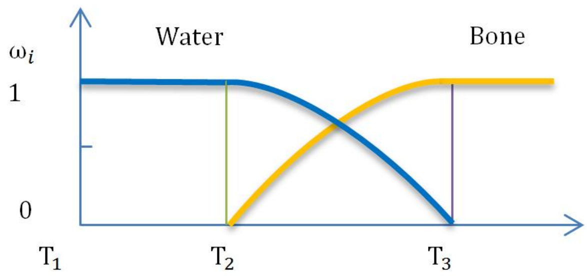

Fig. 3 Weight function distribution

The voxels were assumed to be air equivalent if their CT values fell below threshold T_1, water equivalent if those values fell between T_1 and T_2, bone equivalent if those values fell above threshold T_3, and water-bone mixture if those values fell between T_2 and T_3 (the formula of weight function are shown in Eq. (8) and Eq. (9)).

$$\omega_{\mathrm{water}} = \begin{cases} 1 & \mathrm{T}_1 \le z \le \mathrm{T}_2 \\ \cos^2\left(\frac{\pi}{2}\frac{\mathrm{z}-\mathrm{T}_2}{\mathrm{T}_3-\mathrm{T}_2}\right) & \mathrm{T}_2 < z < \mathrm{T}_3\,, \\ 0 & z \ge \mathrm{T}_3 \end{cases} \tag{8}$$

$$\omega_{\mathrm{bone}} = \begin{cases} 0 & z \le \mathrm{T}_2 \\ \sin^2\left(\frac{\pi}{2}\frac{\mathrm{z}-\mathrm{T}_2}{\mathrm{T}_3-\mathrm{T}_2}\right) & \mathrm{T}_2 < z < \mathrm{T}_3\,, \\ 1 & z \ge \mathrm{T}_3 \end{cases} \tag{9}$$

where z is a pixel CT value.The original image $f(r)$ was segmented into a water image $\omega_{\mathrm{water}} f(r)$ and a bone image $\omega_{\mathrm{bone}} f(r)$ with ω being the weight function and r being the image space coordinates.

Construction of an ideal projection model. The water and bone images were segmented by the proposed method before extracting them through binarization.Then, an ideal projection model was constructed by Radon transform.

Construction of a correction model. The water projection p_w and bone projection p_b were obtained by Radon transform of $\omega_{\text{water}} f(r)$ and $\omega_{\text{bone}} f(r)$. Here, the water image is not pre-corrected and thus has hardening artifacts. The correction model was constructed according to the following formula using the uncorrected water projection data p_w and the bone projection data p_b.

$$p_{final} = \sum_{i=1}^{n-1} c_i p_w^i + \sum_{i=1}^{n-1} d_i p_b^i + \sum_{i=0}^{n} e_i p_w^i p_b^{n-i} . \tag{10}$$

Determination of correction coefficients. In the projection space,the above correction model was compared with the ideal model. The coefficients were determined when the difference was minimal between the two models.

Image reconstruction. The corrected projection was obtained by substituting the corrected coeffcient into the Eq. (9), yielding an image without hardening artifacts.

Experiments

The proposed correction method was verified through simulation and phantom experiments. Taking a 200 mm-diameter water cylinder as the object, the simulation experiment adopts parallel beam scanning and linear array detector. A 0.5 mm copper sheet was added to the outlet location of the ray source (ejection port) to reduce the low-energy part of the spectrum, allowing the maximum number of high-energy energy rays to pass through the object. The energy of the incident photon is negatively correlated with the chance of large angle scattering, as scattering photon is naturally forward-looking. In this way, scattering was effectively suppressed in the simulation experiment. The simulation parameters are shown in Table 1.

Table 1. Simulation parameters

Parameter	Value
Scanning mode	Parallel scan
X-ray energy spectrum, (KeV)	0~100
Attenuation coefficient of Water or bone	NIST's Standard data
Image size, (mm)	Figs. 4-6: 256×256
Detector unit, (mm)	Figs. 4-6: 367

Targeting 200 mm-diameter water phantoms,the phantom experiment relies on a cone-beam spiral CT scanner (Beijing Arrays Medical Imaging Corporation, China). The measurements were performed at a tube voltage of 120 kV for the clinical CT. The proposed method was applied without any assumptions on spectrum, detector, or geometry. For the clinical CT, a 200 mm-diameter water phantom was used in combination with 30 mm-diameter PVC bone rods (SIMONA,Germany). During the simulation experiment, a thorax model is simulated,and three rods were inserted into the water phantom, respectively.

Results and discussion

Correction effect of cupping artifact

The correction effect was verified with simulated polychromatic projection data by Eqs. (2) and (3). It can be seen from the thorax CT image with hardening artifact (Fig. 4(a)) that the middle part had a greater grey value than the outer part, forming a dark area in the centre. This means the image has a serious cupping artifact. Solving the two equation,we have the coefficient matrix c: c = (-0.0000, 0.8042, 0.1462, -0.0342, 0.0033).

Substituting the coefficient matrix into Eq. (5), the corrected projection p_{final} and the corrected image (see Fig. 4(b)) can be obtained.

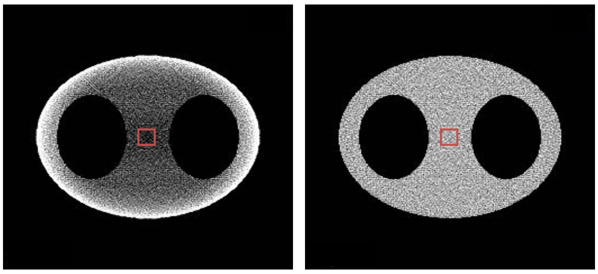

(a) (b)

Fig. 4 (a) Simulation of thorax CT image (b) Corrected water image

Table 2 compares the mean CT value and noise in different regions of interest (ROIs) on the original and corrected images. The attenuation coefficient of each pixel in the 129th colum in both the original image and the corrected image is further compared in Fig. 5.

Table 2. Mean CT value and noise of the original and corrected water images on the ROI

Image	Mean CT value, (1/mm)	Noise, (1/mm)
Original image	0.0210	1.8243e-04
Corrected image	0.0227	2.0032e-04

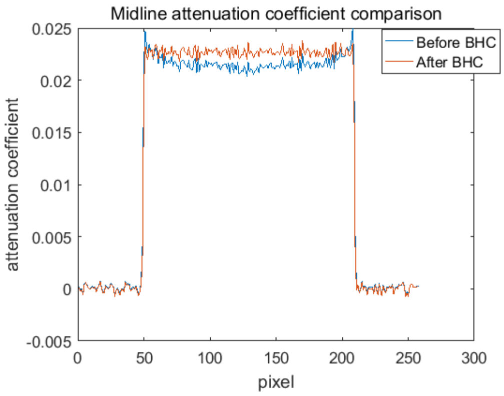

Fig. 5 Comparison of attenuation coefficient

Correction results for streak artifact

Fig. 6(a) shows the original image with three 20 mm-diameter bond rods inserted in the 200 mm-diameter water phantom, in which dark streak artifact can be seen between the high attenuation parts, while using the proposed nonlinear segmentation method and the proposed algorithm using Eqs. (7) and (10), the image corrected (Fig. 6(b)) can be clearly presented.

Table 3 compares the mean CT value and noise in different ROIs on the original and corrected images. In the table, the upper box and the lower box respectively stand for the ROIs in the upper and lower parts.

The proposed method was further evaluated through the phantom experiment on the 200 mm-diameter water phantom inserted with two 30 mm-diameter PVC bone rods. The original image (Fig. 7(a)) has obvious streak artifacts. By contrast, the prominent streaks were not seen in the corrected image (Fig. 7(b)). In addition, the beam hardening correction restored the true CT values. For the water phantom, the mean CT value in the ROIs was corrected from -22 HU to 2 HU.

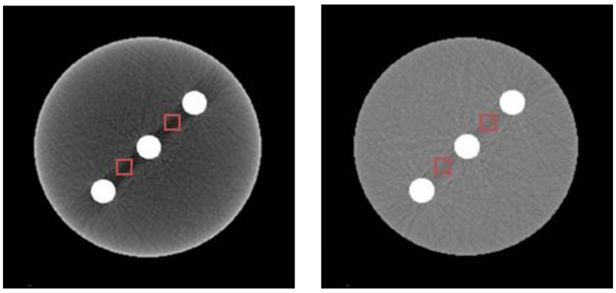

(a) (b)

Fig. 6 (a) Original image with three 20 mm-diameter bone rods inserted in the 200 mm-diameter water phantom; (b) Corrected image

Table 3. Mean CT value and noise of the original and corrected images

Image	ROI	Mean, (1/mm)	Noise, (1/mm)
Original image	Upper box	0.0237	5.9632e-04
	Lower box	0.0238	6.4356e-04
Corrected image	Upper box	0.0262	3.7056e-04
	Lower box	0.0262	3.8638e-04

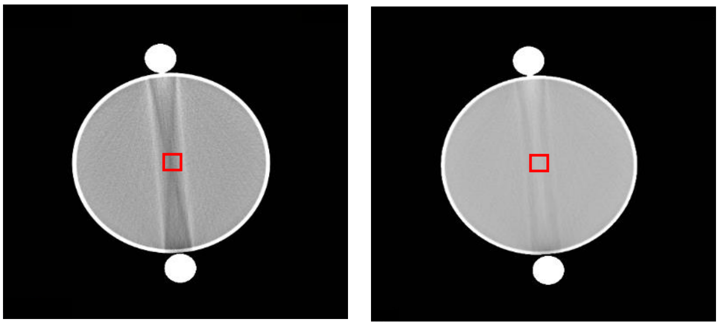

(a) (b)

Fig. 7 (a) Original image with two 30 mm-diameter bond rods inserted in the 200 mm-diameter water phantom; (b) Corrected image

In order to compare the corrective effect of the proposed method based on non-linear segmentation, we also performed the correction method based on linear segmentation. In this phantom experiment, both methods can eliminate the artifacts, and the CT value on the ROI is all corrected from the original -22 to 2, by contrast, the corrected image based on the proposed non-linear segmentation correction method contains smaller noise (Table 4). The corrected curve based on non-linear segmentation is more uniform, as followed in Fig. 8. This is mainly due to the fact that the attenuation of the bone is greater than the attenuation of the water when the water bone is mixed in equal proportion. This non-linear segmentation method is more in line with the attenuation law,while the general linear segmentation ignores this point.

Corrected images were obtained by different segmentation correction method. As can be seen in Table 4, the mean CT value and noise of interest were compared with the original and corrected images. Fig. 8 compares the CT value of each pixel in the middle row of both the original image and the corrected image.

Table 4. Mean CT value and noise of the original and corrected images on the ROI

Image	Mean, (HU)	Noise, (HU)
Original image	-22	113.2234
Corrected image (based on non-linear segmentation method)	2	16.3379
Corrected image (based on linear segmentation method)	2	35.0985

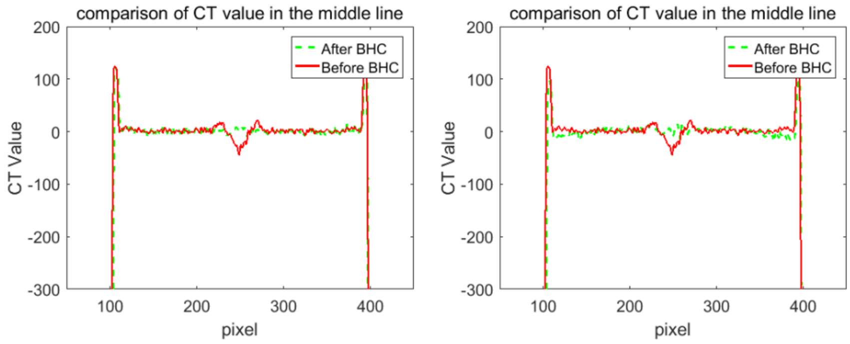

(a) non-linear segmentation correction method

(b) linear segmentation correction method

Fig. 8 Comparison of the CT value of each pixel in the middle row

Conclusion

This paper develops a simple and fast method to remove the hardening artifacts in reconstructed images, and validates the method through simulation and phantom experiments. According to the analysis, the non-linear segmentation method proposed in this paper is more reasonable, which is the premise of correct correction. In this paper, the rationality of non-linear segmentation beam hardening correction method is verified by experiments, and the advantages are obvious.

Compared with the method in reference [2], our method costs a short time and requires a low computing load, because it does not need to transform the projection into the image space. What is more, a one-off image reconstruction is needed in our method, which greatly suppresses the level of noise.

The leading advantage of the proposed method lies in the correction of beam hardening artifacts without prior information of tube spectra, detector efficiency, or even attenuation coefficients. The performance is comparable to or better than that of beam hardening correction in the image space mentioned in references [2, 12].

Disadvantage of the study is that the proposed method is not tested with images of patients, in the next study, we should validate proposed method with patient data.

Acknowledgements

This paper is supported by: National Natural Science Foundation of China (11104058); National Basic Research Program of China (2011CB707500); Natural Science Foundation of Hebei Province (A2011201155); Major Scientific Instruments Program of Ministry of Science *and Technology of China (2011YQ03011405); Key Projects of the Hebei Provincial Education Department (ZD2015044); Key Research and Development Plan of Ministry of Science and Technology of China (2016YFC0104203).*

References

1. Kachelrieß M., K. Sourbelle, W. A. Kalender (2006). Empirical Cupping Correction: A Frst-order Raw Data Precorrection for Cone-beam Computed Tomography, Medical Physics, 33(5), 1269-1274.
2. Kyriakou Y., E. Meyer, D. Prell (2010). Empirical Beam Hardening Correct (EBHC) for CT, Medical Physics, 37(10), 5179-5187.
3. Li D. (2012). Beam Hardening of Correction Algorithm Based on CT System, Chongqing, Chongqing University.
4. Lian Y. Q. (2009). The Algorithms Study of Beam-hardening Correction, Taiyuan, Northwest University.
5. Maass C., E. Meyer, M. Kachelriess (2011). Exact Dual Energy Material Decomposition from Inconsistent Rays (MDIR), Med Phys, 38(2), 691-700.
6. Marshall W. H., R. E. Alvarez, A. Macovski (1981). Initial Results with Prereonstruction Dual-energy Computed Tomography, Radiology, 140(2), 421-430.
7. Nalcioglu O., R. Y. Lou (1979). Post-renconstruction Method for Beam Hardening in Computed Tomography, Physics in Medicine and Biology, 24, 330-340.
8. Shanghai Lianying Medical Technology Co, Ltd (2013). A Correction Method of Bone Hardening Artifacts in CT Image Reconstruction in Chinese, CN 103186883 A.
9. Van Gompel G., K. Van Slambrouck, M. Defrise, K. J. Batenburg, J. de Mey, J. Sijbers (2011). Iterative Correction of Beam Hardening Artifacts in CT, Medical Physics, 38(S1), S36-S49.
10. Wang W., G. P. Li, X. D. Pan, Y. B. Wang (2014).The Simulation of Cone Bone Beam X-ray Spectrum and Intensity Distribution of X-ray in Industrial CT System, Nondestructive Testing, 36(03), 9-13.
11. Zhang X. S., B. S. Zhao (2016). Cupping Artifacts Calibration in CT Image Based on Radon Transform, CT Theory and Applications, 25(5), 539-546.
12. Zhang Y. H., C. Zhang, X. D. Pan (2017). The Methods for Beam Hardening Correction of Cone-beam Industrial Computed Tomography, Nondestructive Testing, 39(6), 8-12.
13. Zhao Y. S. (2015). Iterative Beam Hardening Correction for Multi-material Objects. Chinese Society for Stereology, Proceedings of the Fourteenth China Academic Conference on Stereology and Image Analysis, Chinese Society for Stereology, 9.

Xiaoke Zhang, M.Sc.
E-mail: 1254395643@qq.com

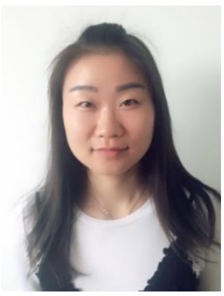

Xiaoke Zhang, female, has Master' degree of Instrumental Science and Technology from the College of Quality and Technical Supervision of Hebei University. Her main scientific interests are in CT image reconstruction and artifact correction research.

Assoc. Prof. Linyan Xue, Ph.D.
E-mail: lyxue@hbu.cn

Linyan Xue, female, Ph.D., is an Associate Professor at the College of Quality and Technical Supervision, Hebei University. Her main scientific interests are in advanced visual cognitive function of the brain-neural mechanism of visual attention; information processing mechanism of brain-computer interface; development of tomography technology and related test instruments.

Kang Yin, M.Sc.
E-mail: 1182856376@qq.com

Kang Yin, male, has Master' degree of Instrumental Science and Technology from the College of Quality and Technical Supervision of Hebei University. His main scientific interests are in the design of acquisition and control system for Micro-CT based on FPGA.

Tianyi Wang
E-mail: wty@china-cas.org

Tianyi Wang, male, Director of the Technology Development Department of the China Association for Standardization. His main scientific interests are in the research work of standardization disciplines.

Assoc. Prof. Kun Yang, Ph.D.
E-mail: hbuyangkun@163.com

Kun Yang, male, Ph.D., is an Associate Professor, Associate Dean, and Master's degree supervisor teacher, at the College of Quality and Technical Supervision, Hebei University. His main scientific interests are in basic theory and applied research of biomedical engineering technology. His research direction is towards basic application and equipment development of molecular medical imaging (PET/CT, SPECT) technology.